Measurement Considerations for Exported Force and Torque Testing of the Ricor K508N Cryocooler

Bill Zwolinski[*], Pascal Erne[**], Lucas Anderson[***], Joel Mork*** and Ian McKinley[****]

Abstract

This paper presents a review of the practical design considerations in the mechanical characterization of micro-vibrations via Exported Force and Torque (EFT) testing. The concepts of piezoelectric force measurement will be discussed along with vibration fixture design, sensor mounting, signal conditioning, and data acquisition. The Active Thermal Architecture (ATA) system will be used as an application example for the EFT characterization of micro-vibrations from a COTS Ricor K508N cryocooler. The ATA employs passive vibration isolation technologies to minimize the impact of vibrational jitter on a suspended kevlar isolated detector. The ATA's use of a Kistler Force Dynamometer, three-axis force transducer, and accelerometer to characterize the multicomponent forces generated by the K508N will be explored and performance benchmarks for the ATA's passive vibration isolation technologies given.

Introduction

Commonly used spacecraft mechanisms span a wide range of applications including cryocoolers for EO/IR imaging, reaction wheels/control moment gyros for attitude control, robotics subsystems as well as actuators, motors, latches and clamps for antennas and positioning/release mechanisms. Exported forces and torque (EFT) resulting from mechanism operation can affect spacecraft mission performance. As such, these disturbances can be continuous vibration or short-term transient depending on the mechanism function. For example, the attitude determination and control system corrects the spacecraft orientation due to exported disturbances without the use of fuel thus creating stable pointing/positioning. Characterization of such EFT-related flight disturbances typically utilizes force dynamometers for multi-component force measurement to characterize micro-vibration disturbances to the spacecraft in 6-components (*Fx, Fy, Fz, Mx, My, Mz)*.

Practical considerations of multi-component force measurement include vibration fixture design, sensor mounting, signal conditioning and data aquisition. For example, factors such as sensor alignment, preloading and checkout/calibration of force test fixtures need to be considered in the design. Force dynamometers are comprised of several sensors where design considerations such as load bearing surface materials, preparation and tolerances as well as mass loading effects are considered for fixture design. Multicomponent force sensor terminology addresses performance parameters such as linearity, hysteresis, cross talk and stiffness to provide an awareness of design considerations as well as FEA and experimental results. As low-level disturbances are to be measured, it is critical to isolate the EFT measurement system from seismic inputs and acoustic noise sources as well as ensuring table resonances are outside the frequency band of interest. As such, measurement noise can be comprised of electrical and environmental effects where noise characterization as a function of analog bandwidths/frequency has to be taken into account. Lastly, depending on the mechanism, vacuum EFT testing may be required to assess mechanism operation where best practices are considered for low outgassing. The results are aimed at achieving a compact design, high frequency, high resolution, and the required dynamic range to characterize the mechanism under test.

[*] Kistler Instrument Corp., Novi, MI bill.zwolinski@kistler.com
[**] Kistler Instrumente AG, Winterthur, Switzerland pascal.erne@kistler.com
[***] Utah State University, Logan, UT lucas.anderson@usu.edu
[****] NASA JPL, Pasadena, CA ian.m.mckinley@jpl.nasa.gov

The Active Thermal Architecture (ATA) system is a sub 1U two-stage, single-phase Mechanically Pumped Fluid Loop (MPFL) active thermal control technology targeted at 6U CubeSat platforms and above. The ATA's first stage comprises a micro-pump-driven MPFL, connecting an internal heat exchanger to a deployable tracking radiator through a two-axis rotary fluid hinge. A COTS Ricor K508N cryocooler forms the second stage and provides cryogenic cooling to a custom Kevlar detector mount. The ATA system utilizes advanced 3D fabrication techniques such as Ultrasonic Additive Manufacturing to miniaturize and simplify the MPFL by directly embedding the working fluid channels into the CubeSat chassis. The ATA system includes passive vibration isolation and damping technologies such as wire rope isolation, particle dampers, and flexible (TMT) pyrolytic graphene thermal straps to mechanically isolate the active components from the CubeSat and payload and to minimize the impact of micro-vibrations on mission success. [1]

Funded by the NASA Small Spacecraft Technology Program, the ATA project is a joint venture between the Center for Space Engineering at Utah State University and the NASA Jet Propulsions Laboratory. It is a continuation of the Active CryoCubeSat Project project. The ATA technology as been selected for demonstration on the Active Cooling for Multi-spectral Earth Sensors (ACMES) mission scheduled to launch in late 2024. The ATA will act as thermal support for the University of Hawaii's Hyperspectral Thermal Imaging instrument (HyTi). This flight is funded through the In-Space Validation of Earth Science Technologies (InVEST) program and the Earth Science Technology Office (ESTO). [2]

Piezoelectric Force Technology - Concept of Operation

Piezoelectric (PE) sensors make use of the piezoelectric effect of single crystals such as quartz (SiO_2), in which the charge released is proportional to the applied load. Because natural quartz crystals contain too many imperfections, use is made of quartz grown artificially under precision-controlled conditions. Quartz crystals are grown artificially in autoclaves as illustrated in Figure 1. [3], [4]

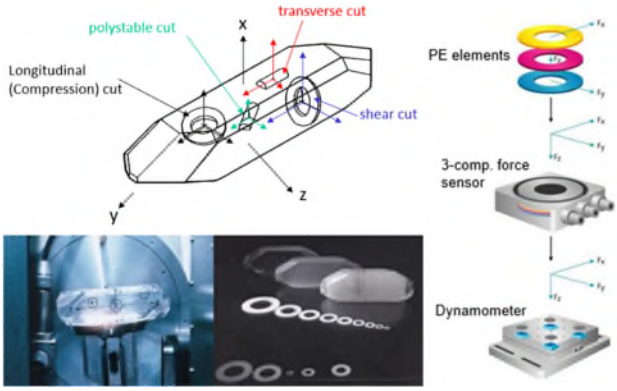

Figure 1: Illustration of Quartz Crystal and use in 3-Component Force Sensors and Force Dynamometers

Quartz sensors provide high stiffness and quasi-static to high-frequency operation nature demonstrates that the sensitivity of quartz remains extremely stable: natural quartz that is over one million years old retains the same pC/N sensitivity, with virtually no sensitivity shift over its lifetime. Kistler also grows its own high-performance crystals known as PiezoStar®, which has higher sensitivity and higher operating temperature compared to quartz.

Piezoelectric Terminology

PE sensors do not have internal electronics, so they require an external charge amplifier to convert the electrical charge signal into a proportional voltage. An IEPE (Integrated Electronic Piezoelectric) sensor, however, does have internal electronics powered by a constant current supply, thus providing a voltage output. Figure 2 compares the properties of PE and IEPE sensors. EFT systems commonly use PE technology.

	PE (pC/mu) - Piezoelectric	IEPE (mV/mu) - Integrated Electronics Piezo Electric
Electronics	External charge amplifier	Internal charge to voltage converter, powered by IEPE constant current supply
Cable	High impedance	Standard cable
Temperature	Very wide range	Limited with integrated electronics
Rangable	Yes.	No.
Measurement	Quasi-static (long TC) as well as highly dynamic measurements possible	Only dynamic.
Reset/Measure	Tares the measurement to remove static loads from the dynamic range	Not possible
TEDS	n.a. (retrofit only)	Yes

Figure 2: Comparison of PE and IEPE Piezoelectric Sensors Types

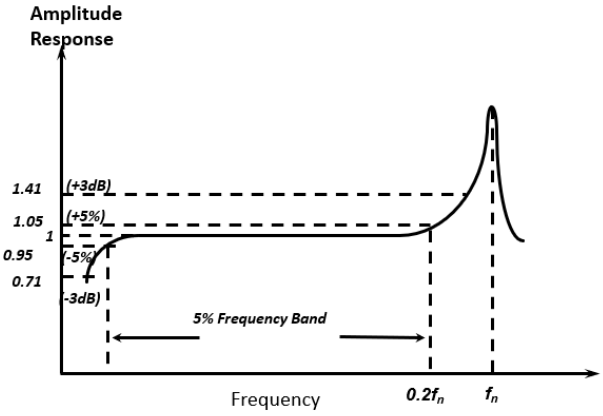

Approximation for PE Sensors

$f_{5\%} \sim f_n/5$; $f_{10\%} \sim f_n/3$; $f_{3dB} = f_{+41\%} \sim f_n/2$

Figure 3: Typical Frequency Response of a PE Sensor

Piezoelectric Sensor Frequency Response

A PE sensor can be described as a lightly damped second-order system at medium to high frequencies, and as a single-order high-pass characteristic at low frequencies, as illustrated in Figure 3.

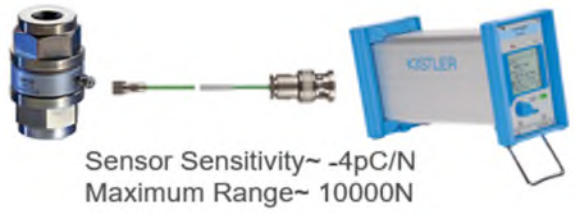

Full Scale Range (FSR = 10V)	Output Scale Factor (N/V)	Broadband Noise rms	Broadband Noise rms
1 N	0.1 N/V	0.0045 Vrms	0.00045 Nrms
25 N	2.5 N/V	0.0012 Vrms	0.003 Nrms
1000 N	100 N/V	0.0006 Vrms	0.06 Nrms
10000 N	1000 N/V	0.0006 Vrms	0.6 Nrms

Figure 4: PE Measuring Chain Rangeability Example

Piezoelectric Measuring Chain Rangeability

The PE measuring chain is rangeable using an external charge amplifier where noise (resolution) scales as a function of the selected measuring range. Figure 4 shows an example of the noise (resolution) as a function of the selected range. The rms (root mean square) noise is the integration of noise power spectral density over operational frequency range. The Reset/Measure function of the amplifier also allows taring of the measuring chain from a static mass acting on it.

Design of PE Force Dynamometers

Non-axial forces applied to an individual force sensor create moment loads which at best degrade accuracy and, at worst, can break the sensor. A PE force dynamometer comprises an array of force sensors mounted between thick metal plates. Important parameters to be considered and related to performance are the parallelism of the cover and base plate, flatness, strength and stiffness. The better these parameters are, the better the frequency response will be. A certain minimum tensile strength is necessary so that the top and bottom plate can withstand the large forces from the preloading bolt.

Figure 5: Example of a Ceramic Micro-Vibration Dynamometer Type 9236A2

Force dynamometers absorb non-axial loads and distribute moment loads by differential force reactions within the force sensor array; they can be of various shapes and sizes – square, triangular, rectangular, or circular. A PE force dynamometer measures the magnitude and direction of *Fx, Fy, Fz* acting on the dynamometer, but it does not measure their spatial location on the top plate. [5]

A search for new materials for the top plate found ceramic offers highly advantageous properties for EFT, low specific gravity and a high modulus of elasticity. Finite element method calculations show that natural frequencies are increased by 40% for ceramic top plates

with the same dimensions as steel. This is especially important for large test articles and corresponding large dynamometers.

Typically, four force sensors are used between two parallel plates to calculate the 6 components forces and moments. A typical dynamometer geometry is shown in Figure 6. As shown a, b is the vertical and horizontal separation relative to the force sensor center to dynamometer center line respectively.

$$F_x = F_{x1+2} + F_{x3+4} \quad (1)$$

$$F_y = F_{y1+4} + F_{y2+3} \quad (2)$$

$$F_z = F_{z1} + F_{z2} + F_{z3} + F_{z4} \quad (3)$$

$$M_x = b * (F_{z1} + F_{z2} - F_{z3} - F_{z4}) \quad (4)$$

$$M_y = a * (-F_{z1} + F_{z2} + F_{z3} - F_{z4}) \quad (5)$$

$$M_z = b * (-F_{x1+2} + F_{x3+4}) + a * (F_{y1+4} - F_{y2+3}) \quad (6)$$

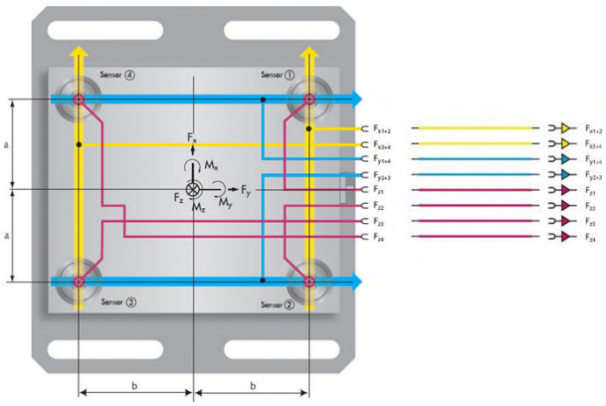

Figure 6: *Dynamometer Geometry with 4x 3-Component Force Sensors Resulting in 6-Component Equations for Fx, Fy, Fz, Mz, My, Mz*

A PE dynamometer can be represented as a simple spring mass model consisting of:

- A base plate
- A top plate with mass *m*
- A spring with stiffness k_f
- A damper with damping coefficient *D*

PE sensors and dynamometers usually have very low damping (0 < *D* < 0.01). The large cross-section of the quartz plate sensing elements for the 3-component sensor results in very high stiffness which supports high-frequency measurements. Even with an additional mass, the natural frequency of a PE dynamometer remains high due to the equivalent stiffness. The dynamometer exhibits the same behavior as a lightly damped second-order system (see Figure and Figure). Added mass acts to reduce the natural frequency, as illustrated. [6]

$$f_r = \frac{1}{2\pi} \cdot \sqrt{\frac{k_f}{m}} \quad (7)$$

$$f_{r,red} = \frac{1}{2\pi} \cdot \sqrt{\frac{k_f}{m + m_2}} \quad (8)$$

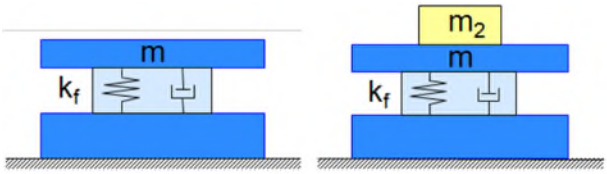

Figure 7: Spring Mass Model of PE Dynamometer

m: mass of top plate
k_f: stiffness of spring
m_2: added mass
$f_{r,red}$: reduced resonance frequency

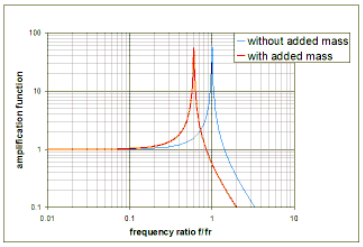

Figure 8: Natural Frequency of Spring Mass System

<u>Analog bandwidth considerations relating to measurement</u>

For PE force measurement the charge amplifier determines lowest and highest frequencies that can be measured. The test article and application define the required frequencies of interest and associated resolution. However, the test stand, fixtures and mass acting upon the PE force dynamometer determine the highest possible measurement frequency. As the amplitude response tolerances can be expressed as a function of natural frequency the 5%, 10%, 3 dB bandwidths can be selected to make the measurement.

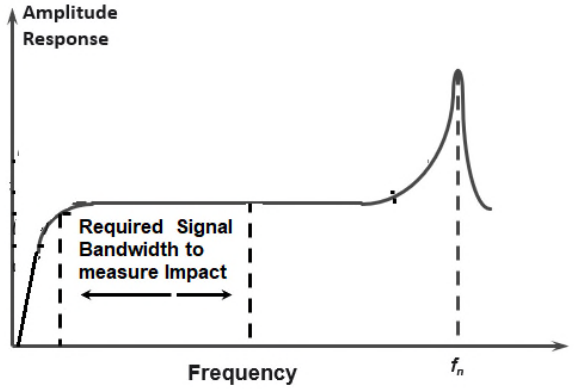

Figure 9: Illustration of Required Signal Bandwidth and Force Sensor Natural Frequency

Design Drivers for Operational Performance Testing of Reaction Wheels

With reaction wheel testing, the magnitude and frequency of a wheel's EFT is characterized. A reaction wheel test dynamometer consists of four 3-component force sensors. The output of each of the sensors are summed in *Fx*, *Fy* and *Fz* for the resulting impact forces where moments can be calculated as described in equation (4) - (6). The PE force dynamometer has a very large measurement range and is rangeable allowing for measurements for very small reaction wheels. As a result, one PE dynamometer size will fit all measurement requirements. High natural frequency, also in shear direction is required where the dynamometer must also provide a stiff interface with easy mounting possibilities. Lastly the PE dynamometer uses a charge amplifier for rangeability, high dynamic range and high signal fidelity.

Typical dynamometer installation guidelines

As shown in Figure 10, the dynamometer is hard-mounted on the seismically isolated table and the test article is hard-mounted on top of the dynamometer. The top adapter plate is typically made of aluminum; it mates with the hole pattern of the dynamometer and has the hole pattern required for the test article. The bottom adapter plate mates with the hole patterns of the table and of the dynamometer. Maintenance of 0.01 mm flatness and parallelism of the adapter plates is recommended for the best frequency response. The bottom adapter plate can sometimes be eliminated if the table has the same mounting hole pattern as the dynamometer: direct mounting is then possible. Again, the table surface should be flat and parallel to within 0.01 mm. Granite or optical tables provide a stiff and rigid mounting surface so that resonances are minimized, ideally remaining outside the measurement frequencies of interest.

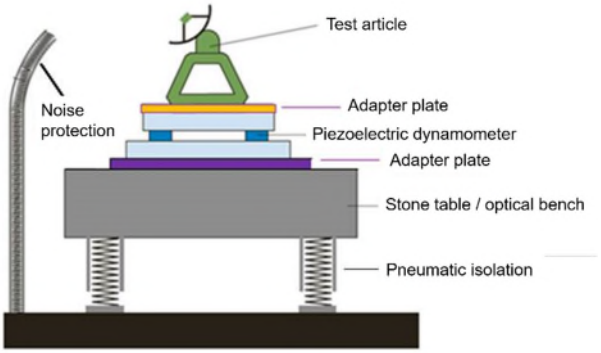

Figure 7: Typical Installation of Dynamometer for EFT Testing

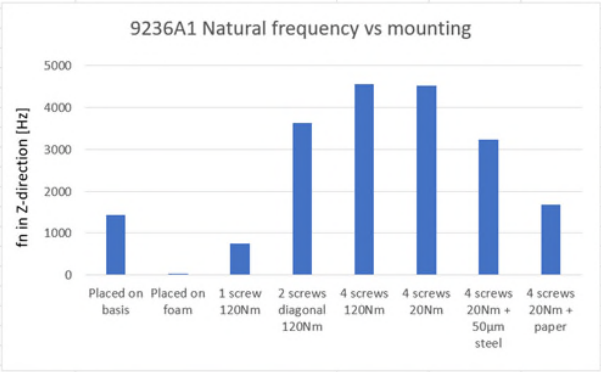

Figure 8: Effect of Frequency Response for Various Mounting Parameter such as Torque, Flatness, and Number of Fasteners

For granite or stone tables, the general rule is that the mass mounted on the test bench is less than 10% of the table's mass. As mentioned above, acoustic noise protection is also recommended for the installation. The background vibration (noise) for the facility/table setup can be determined by running an ambient noise test once the dynamometer is connected and the overall setup is completed.

As Figure 11 shows, it is more important to ensure flatness, parallelism, and an adequate number of fasteners than to achieve the highest preload. In the ideal mounting configuration, the dynamometer is fastened on the base with four screws (measurement 5). The effect of mounting torque is small (there is almost no difference between 120 N·m and 30 N·m torque for mounting screws). Since fewer fasteners

and less surface flatness can degrade the frequency response, any configurations other than measurement 5 are not recommended.

Data Acquisiton

Depending on the signal to be measured, AC coupled, or DC coupled data acquisition is used. EFT charge amplifiers are typically set up in short or medium time constant as EFT is an AC coupled measurement. With today's 24-bit data acquisition systems, the resulting measurement resolution is usually far greater than is required for the signal measurement. Bandwidth is the difference between the upper and lower frequency in a continuous band of frequencies; theoretically, the minimum sample rate is two times the maximum signal frequency but in practice, 5 to 10 times is used to avoid aliasing. For this purpose, the natural frequency of the complete system (including force sensors and fixtures, etc.) must be considered.

Noise consideration

Noise consists of unwanted random fluctuations that degrade signals and limit the minimum signal level that can be measured. The total noise from multiple random (white) noise sources can be described as:

$$\sigma_{rms} = \sqrt{{\sigma_1}^2 + {\sigma_2}^2 + \cdots + {\sigma_N}^2}. \qquad (9)$$

Filtering reduces noise and enhances the signal quality but can affect the overall analog bandwidth of interest.

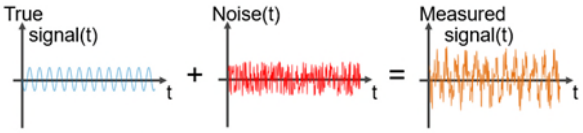

Figure 9: Schematic of a Measurement Signal Affected by Noise

Electrical noise can adversely affect the measurement noise. Use of ground-isolated measuring chains is preferred to avoid ground loops where one common ground for the measurement chain is provided. EFT Dynamometers are typically ground isolated complementing low noise measurement.

Avoiding strong electromagnetic fields (e.g., electromagnetic interference (EMI)) in the area of the instrumentation/cables is best practice, as is the use of 360°-shielded cables. The battery power of the signal conditioner and amplifiers can often show an improvement in both noise level and 50 Hz/60 Hz harmonics due to the AC-DC power conversion process, which is not a perfect process. Lastly, analog bandwidth is proportional to root mean square (RMS) noise.

Multi-channel charge amplifiers with internal summing calculators generate some additive electrical noise to the measured 6-components. Using software (such as DynoWare) to compute the six component signals from the component signals results in no additive noise compared to the internal summing calculator. Additional noise error sources originating from the environment include HVAC inputs with airflow on structures under test, acoustics, structure-borne noise, structural response of the test rig or transmissibility of seismic inputs to the sensors performing the measurement; we will not discuss these sources in this paper, but they must nevertheless be taken into account.

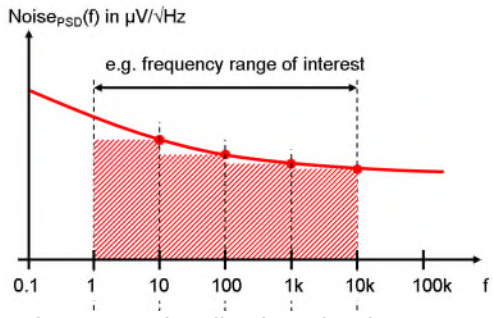

Figure 10: Visualisation of Noise Power Spectral Density

Noise power spectral density

The noise power spectral density describes the signal's power content versus frequency. It allows the noise to be estimated as a function of bandwidth/filtering. Fast Fourier Transform (FFT) is effectively narrowband filtering of the signal of interest. Narrowband FFT processing can support higher resolution and signal-to-noise ratio on a frequency bin basis, where the frequency bin width is related to the number of FFT points and sample rate. The noise RMS can be calculated as:

$$\text{Noise}_{rms} = \sqrt{\int_{f_L}^{f_H} [\text{Noise}_{PSD}(f)]^2 df}. \qquad (10)$$

Calibration

Calibration not only provides information about the functionality of the measuring equipment, but also precisely determines characteristics such as sensitivity, linearity, hysteresis, crosstalk and drift, and thus contributes significantly to the overall accuracy of the measurement. Only a fully calibrated measurement chain can provide the necessary confidence in the measurement equipment.

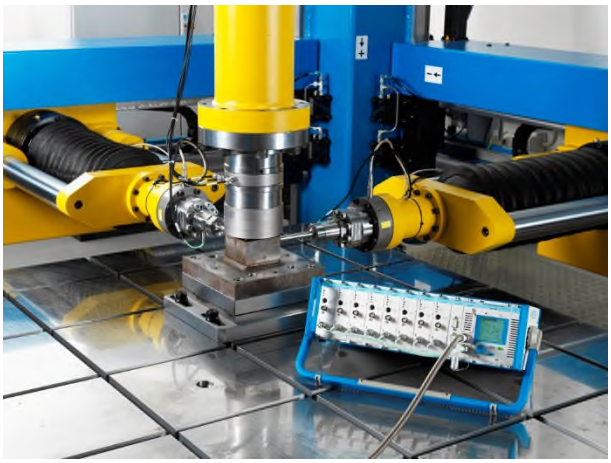

Figure 12: 3-Component Force Dynamometer with 5080A charge amplifier at Calibration

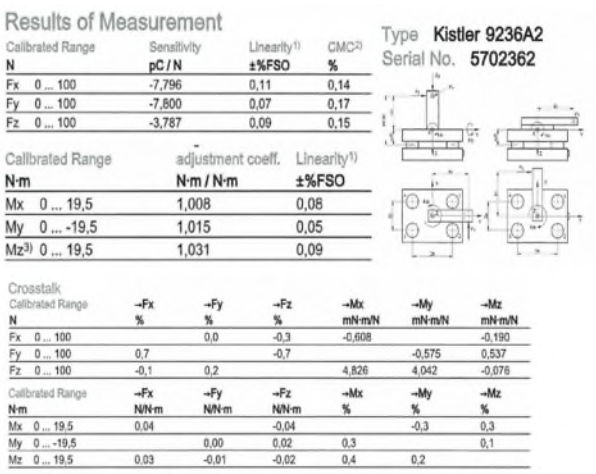

Results of Measurement

Type Kistler 9236A2
Serial No. 5702362

Calibrated Range N	Sensitivity pC / N	Linearity[1] ±%FSO	CMC[2] %
Fx 0 ... 100	-7,796	0,11	0,14
Fy 0 ... 100	-7,800	0,07	0,17
Fz 0 ... 100	-3,787	0,09	0,15

Calibrated Range N·m	adjustment coeff. N·m / N·m	Linearity[1] ±%FSO
Mx 0 ... 19,5	1,008	0,08
My 0 ... -19,5	1,015	0,05
Mz[3] 0 ... 19,5	1,031	0,09

Crosstalk

Calibrated Range N	→Fx %	→Fy %	→Fz %	→Mx mN·m/N	→My mN·m/N	→Mz mN·m/N
Fx 0 ... 100		0,0	-0,3	-0,608		-0,190
Fy 0 ... 100	0,7		-0,7		-0,575	0,537
Fz 0 ... 100	-0,1	0,2		4,826	4,042	-0,076

Calibrated Range N·m	→Fx N/N·m	→Fy N/N·m	→Fz N/N·m	→Mx %	→My %	→Mz %
Mx 0 ... 19,5	0,04		-0,04		-0,3	0,3
My 0 ... -19,5		0,00	0,02	0,3		0,1
Mz 0 ... 19,5	0,03	-0,01	-0,02	0,4	0,2	

Figure 11: Example of a Calibration Certificate incl. Crosstalk and Linearity

Figure 14 shows the calibration test stand where calibration is performed using a multi-component press for high loads as illustrated below. In each axis there is a strain gage sensor to control the applied force and a PE force sensor to quasi-statically calibrate the PE dynamometer in *Fx, Fy* and *Fz*. Figure 15 shows the calibration results indicating very low crosstalk and highly linear operation of the multicomponent PE force platform.

Application – Ricor K508N Micro-Vibrations for the ATA system

Understanding the impact of micro-vibrations on spacecraft structures and payloads can be mission critical. For example, micro-vibrations, or jitter, can cause excitation of the support structures for optical elements during imaging operations, this can result in severe degradation of image quality due to smearing and distortion for Earth observation satellites. A prime example of this is the inclusion of miniature cryocoolers for sub-cooled electro-optical instrumentation on CubeSat platforms. Stirling cryocoolers in particular rely on a dynamic compression stage which can induce high amplitude frequency dependent vibrations that can be detrimental to sensitive optical instruments. The ATA system features an integrated Stirling based Ricor K508N miniature cryocooler. The K508N is a long life tactical cryocooler based on a high-speed rotary compression cycle (reciprocating vibration) and as such generates micro-vibrations. Cryocooler's generally impart body vibrations throughout the satellite structure, as well as cold tip vibration, which can be passed directly to sensitive instrumentation. To mitigate the impact of this jitter on critical systems, the ATA technology features several of passive vibration isolation technologies. Including wire rope spring isolation of the entire ATA system, a cold tip particle damper, and a Pyrolytic Graphene Sheet (PGS) thermal link to mechanically isolate the cryocooler cold tip from the detector assembly. The ATA K508N cryocooler is shown in Figure 16 with industry standard coordinate directions labeled.

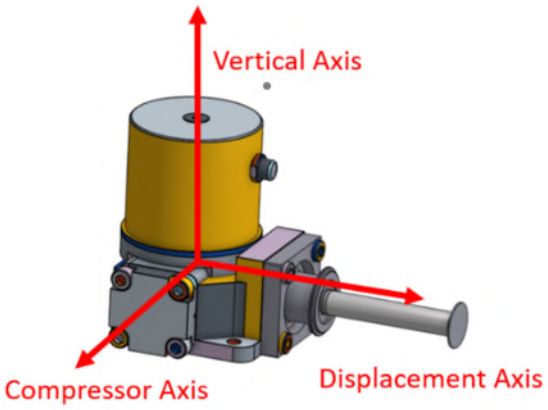

Figure 16: Ricor K508N cryocooler CAD model with common coordinate axis

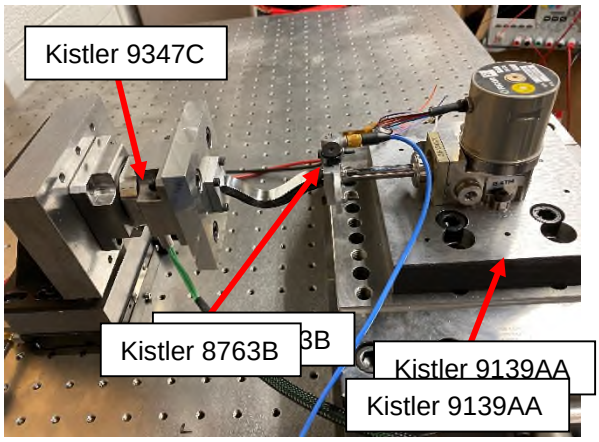

Figure 17: Kistler EFT test setup for the characteriztion of the ATA Ricor K508N micro-vibrations

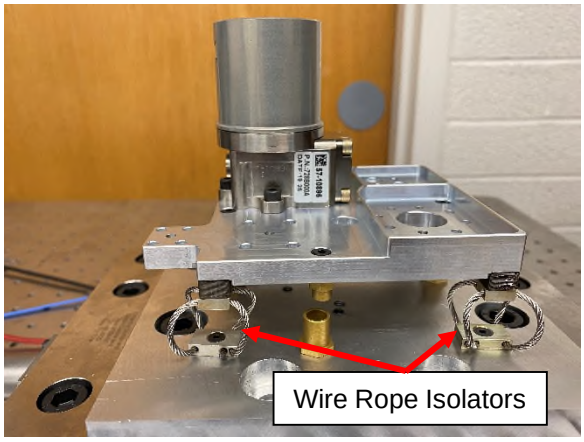

Figure 18: Wire rope isolation of the ATA K508N cryocooler

The ATA K508N cryocooler was simultaneously characterized for body EFT, cold tip exported triaxial force, and acceleration. The integrated K508N cryocooler was mounted to a Kistler 9139AA multi-component dynamometer that provided 6-component equations. Three-axis orthogonal force and three-axis moment measurements. The cryocooler cold tip was attached to a horizontally mounted Kistler 9347C triaxial force transducer. Which directly measured the exported force of the cold tip while an 8763B Kistler low noise accelerometer was also mounted to the cold tip and recorded the triaxial acceleration. Figure 17 shows the ATA cryocooler mounted to the Kistler dynamometer with the Space Dynamics Laboratory TMT PGS thermal link attached to the force transducer. Each of these Kistler EFT sensors were fed into a quasi-static 5080A multi-channel charge amplifier to integrate, convert, and amplify the measurement signal. Four parallel 5165A LabAmp data acquisition cards recorded the frequency dependent multi-component micro-vibration signals from each Kistler instrument at 20 MHz. Kistler DynoWare was used to interface and collect the various signals and process the data to text files. A custom MATLAB code was used to post process the data. The data was low pass filtered and analyzed via Fourier transform. The ATA heat exchanger plate, shown in Figure 18, has four ITT Enidine CR2400BM wire rope isolators attached at each corner. Gold anodized mounting posts are used to lock the heat exchanger down.

The ATA K508N cryocooler exhibits a strong vibration peak at approximately ~80 Hz. This can be seen as the first peak in Figures 19 & 20 for the hard mounted case. This first peak corresponds to the Stirling cycle drive frequency of the K508N and is similar for all cryocoolers tested by the ATA project. From this point, higher order harmonics dominate until close to 1000 Hz. When high frequency noise, likely caused by internal rubbing washes out the signal with white noise. The CR2400BM wire rope isolators have resonant peaks at ~85 Hz (Compressor axis), ~120 Hz (Displacer), and ~400 Hz (Vertical). Unfortunately, the 80-Hz driving signal of the K508N amplifies the wire rope isolator's compressor axis resonance. Therefore, the vibration isolation of the WRI's sees a sharp peak near 80 Hz, in the compressor and vertical axis, and then a rapid damping of all higher-order harmonics and noise. Overall, the wire rope isolators show a significant (several orders of magnitude) reduction in the overall amplitude of the exported force for the K508N EFT.

The PGS thermal strap exhibits a roll off frequency between ~20 & 500 Hz. Higher and lower frequencies do not appear to be dampened as much. The PGS thermal link shows the highest damping in the displacer axis and vertical axis, which corresponds to the directions of most flexibility. Figures 19 & 20 show the exported triaxial force of the cryocooler body and cold tip as measured by the Kistler 9139AA dynamometer and 9347C force transducer. Micro-vibration signals are referenced to hard mounting the cryocooler body and cold tip, as opposed to mechanical isolation via wire rope isolation and PGS thermal link. Further information on the vibrational characterization of the ATA Ricor K508N can be found in Ref [1].

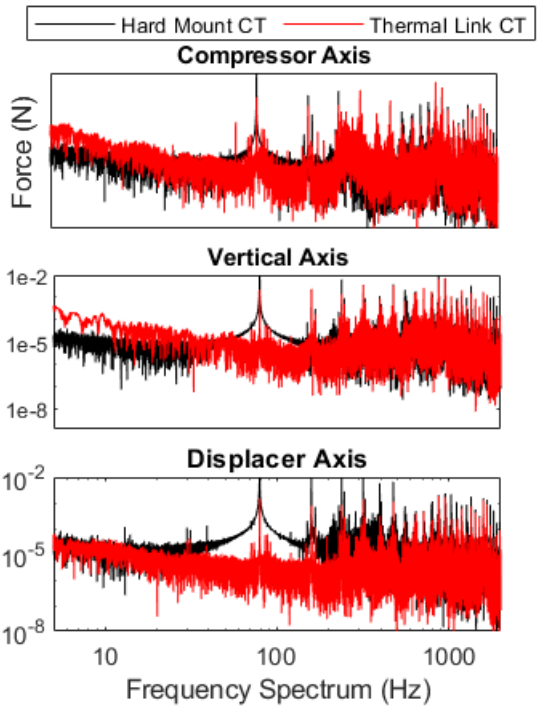

Figure 19: Exported cold tip force for the Ricor K508N. Force comparison of the cold tip hard mounted vs. mechanically isolated via PGS thermal link

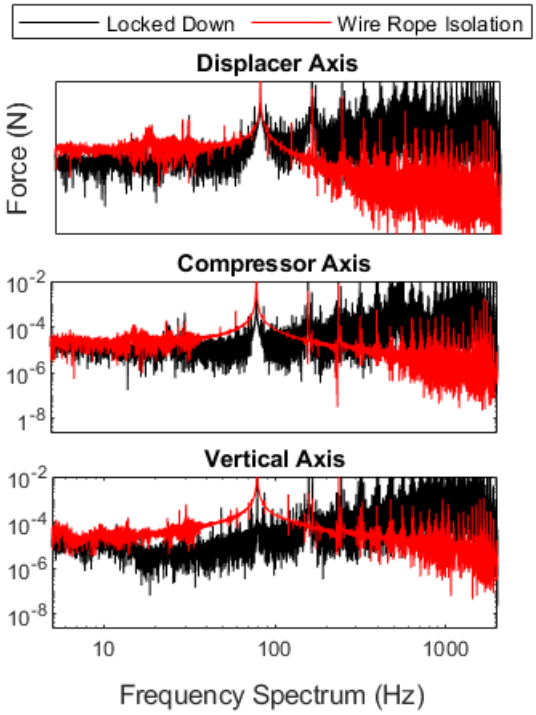

Figure 20: Exported body EFT for the Ricor K508N. Force comparison for hard mounted vs. mechanically isolated via wire rope isolators

Conclusions

Practical considerations for the mechanical characterization of micro-vibrations via Exported Force and Torque testing included vibration fixture design, sensor mounting, signal conditioning, and data acquisition. The Active Thermal Architecture system used a COTS Ricor K508N cryocooler employed passive vibratoin isolation technologies to minimize the impact of vibrational jitter. The EFT system utilized a Kistler Force Dynamometer, three-axis force transducer, and triaxial accelerometer to characterize the multicomponent forces generated by the K508N. The ATA's passive vibration isolation technologies provided an effective method to reduce EFT.

References

[1] L. Anderson, C. Swenson, R. Davidson, A. J. Mastropietro, E. Maghsoudi, S. Luong, S. Cappucci, and I. Mckinley "CubeSat active thermal management in support of cooled electro-optical instrumentation for advanced atmospheric observing missions", Proc. SPIE 10769, CubeSats and NanoSats for Remote Sensing II, 1076907 (18 September 2018); https://doi.org/10.1117/12.2321959
[2] Lucas Anderson, Joel Mork, Charles Swenson, Bill Zwolinski, A. J. Mastropietro, Jonathan Sauder, Ian McKinley, and Mason Mok "CubeSat active thermal control in support of advanced payloads: the active thermal architecture project", Proc. SPIE 11832, CubeSats and SmallSats for Remote Sensing V, 1183203 (2 August 2021); https://doi.org/10.1117/12.2594375
[3] Bill Zwolinski, Pascal Erne (2021). Practical Consideration in multicomponent force measurement for mechanism exported force and torque (EFT) testing
[4] Force Sensors, Kistler, 960-350e-4.0 © 2019 Kistler Group https://www.kistler.com/files/download/960-262e.pdf
[5] Christof Sonderegger (2017). Tracking Micro-vibrations. Micro-vibration testing. Showcase 2017. Aerospacetestinginternational.com, pp 78-81.
[6] Paul A. Tipler and Gene Mosca. “Physik – Für Wissenschaftler und Ingenieure" (2004): pp. 246
[7] L Anderson1 , J Mork1 , C Swenson1 , B Zwolinski2 , A J Mastropietro3 , J Sauder3 , I McKinley3 and M Mok3 “Random vibration, exported vibration, and passive isolation testing of the Ricor K508N cryocooler” Cryocooler Engineering Conference, CEC, 2021